ChemComm

Accepted Manuscript

This article can be cited before page numbers have been issued, to do this please use: Y. Cui, X. Feng, X. Li, Y. Zhang, A. Tang and D. Kong, *Chem. Commun.*, 2019, DOI: 10.1039/C9CC03758F.

ROYAL SOCIETY OF CHEMISTRY

rsc.li/chemcomm

View Article Online
DOI: 10.1039/C9CC03758F

COMMUNICATION

Trifunctional Integrated DNA Based Universal Sensing Platform for Detection of Diverse Biomolecules in One-pot Isothermal Exponential Amplification Mode

Received 00th January 20xx,
Accepted 00th January 20xx

DOI: 10.1039/x0xx00000x

Yun-Xi Cui[a,b,†], Xue-Nan Feng[a,†], Xiao-Yu Li[a], Yu-Peng Zhang[a], An-Na Tang[a], De-Ming Kong[a,b,*]

A BIOSENSOR WITH ALL ADVANTAGES OF ULTRA-HIGH SENSITIVITY, EASE-TO-OPERATION, STRAIGHTFORWARD SIGNAL OUTPUT AND UNIVERSAL APPLICABILITY HAS BEEN INTRODUCED. SUCH BIOSENSOR WAS DEMONSTRATED TO WORK WELL IN DETECTION OF POLYNUCLEOTIDE KINASE AND DAM METHYLTRANSFERASE, THUS PROVIDING POWERFUL TOOLS FOR CLINICAL DIAGNOSIS, DRUG SCREENING AND DISEASE THERUPIC ASSAY.

During the development of the modern biological science, different biomolecules, such as the nucleic acids, proteins and enzymes, have attracted intense interest because of the identification for the vital impact of those molecules in various bio-processes[1-6]. It has been reported that the abnormal expression of some biomolecules was closely related with numerous of diseases[7-13]. In light of the clinical significance of those biomolecules, they are applied as series of biomarkers in diagnosis and prognosis[14]. Therefore, developing of a convenient and sensitive strategy, for the rapid detection of those biomarkers with high sensitivity, has definitely great potential in biology and bioanalysis.

DNA has been applied as a powerful tool for design of biosensors because of its predictable and programmable sequences, as well as their ability to replicate with ultra-high efficiency[15-19]. In recent decade, plenty of DNA-based biosensors have been developed for analysis of different biomarkers, including nucleic acids, enzymes or other molecules which can be used as the special targets of DNA aptamers[20-27]. In order to achieve the detection of molecules in extremely low concentration, researchers introduced multiple signal amplification steps in the design of the biosensors[28-31]. For instance, the polymerase chain reaction (PCR) is a well-known method that has been widely applied in construction of different biosensors[32]. However, the processes of PCR request to set up programmed temperature cycles, and a denatured temperature as high as 95°C is necessary[33]. The complicated processes limit the application of PCR in analysis of biomolecules, especially for those in natural samples. Therefore, isothermal amplification methods attracted more and more attention. Nevertheless, comparing with the canonical PCR, the efficiencies of the isothermal amplification methods are usually lower so their sensitivity is not as high as conventional PCR. To achieve the detection of low abundance biomolecules, people attempted cascade amplification strategies which included multiple reaction steps to ensure the high sensitivity[7, 34, 35]. But the more steps not only make the operation more complicated, but also increase the risk of cross-contamination between the materials.

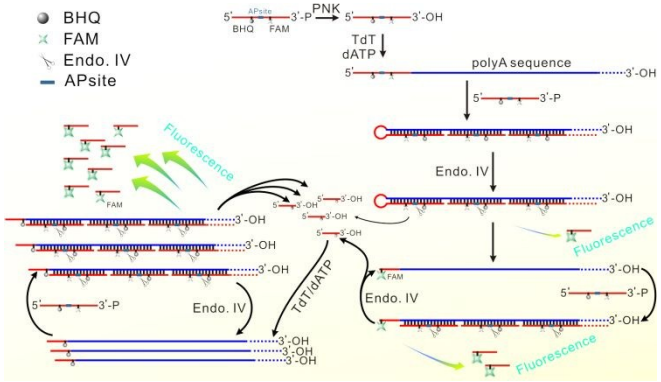

Scheme 1. Mechanism of the PARTIP for detection of PNK activity.

Herein, we proposed a novel DNA-based biosensor, named Probe-Amplifier-Reporter Trifunctional Integrated Platform (or termed as PARTIP). The PARTIP is constructed with only one DNA substrate. This single-stranded DNA plays 3 roles of probe, amplifier and reporter. In the presence of the target, multiple amplification processes will be initiated spontaneously, achieving detection of the target with ultra-high sensitivity. Notably, although multiple amplification processes are included in, the overall procedures can be completed in a simple "one-pot" mode because all of the reactions proceeded synchronically. What's more, the single-stranded DNA substrate can be easily modified for recognition of different biomolecules, thus the PARTIP may be extended as a general sensing platform for detection of diverse biomarkers. As a proof of concept, we designed two PARTIP sensors for analysis of polynucleotide kinase (PNK) and Dam methyltransferase (Dam MTase). PNK is a kind of kinase that plays an important role in various gene-related bioprocesses, such as DNA replication, DNA repair, and nucleic acid metabolism[36-38], and the MTase was found to related with several types of cancer[6, 39]. Our results suggested

[a] State Key Laboratory of Medicinal Chemical Biology, Tianjin Key Laboratory of Biosensing and Molecular Recognition, Research Centre for Analytical Sciences, College of Chemistry, Nankai University, Tianjin 300071, P R China
[b] Collaborative Innovation Center of Chemical Science and Engineering (Tianjin), Tianjin, 300071, P R China.* E-mail: kongdem@nankai.edu.cn. Fax: +86-22-23502458.
† These authors contributed equally.
Electronic Supplementary Information (ESI) available: Experimental Section and supplementary Figures S1-S11, See DOI: 10.1039/x0xx00000x

that the PARTIP could be applied in the detection of these two cancer-related enzymes in an ultra-simple and high-sensitivity way.

As shown in **Scheme 1**, our design applied a 20 nt long, single-stranded poly-thymine (pT) DNA as the basic substrate (pT). For PNK detection as an example, the substrate was modified with a 3'-phosphate (3'-P) end, and an apurinic/apyrimidinic (AP) site in the middle. A fluorophore-FAM and a black-hole quencher (BHQ) were pre-labeled at each side close to the AP-site, forming the pT_{PNK} substrate. The PNK might catalyze the 3'-end dephosphorylation of pT_{PNK}, converting the 3'-P end to 3'-OH[22]. And the generated 3'-OH end could be recognized and elongated by terminal transferase (TdT), a kind of DNA polymerase without substrate sequence selectivity[40]. We introduced dATP only for the TdT-catalyzed elongation reaction, thus the long-tail product would be a poly-adenine (pA) sequence. The pT_{PNK} strands, either reacted with PNK/TdT or not, may hybridize with the pA tail, forming multiple intra/inter-molecule duplexes. Each duplex contained a pre-set AP-site in the middle, at which the pT_{PNK} strand would be cut into two short parts by Endonuclease IV (Endo. IV). Due to the great decrease of the binding stability (melting temperature decreased from 53.1 °C to 28.5 °C, calculate using *mfold*[41]), the two parts could not form stable duplexes with the pA tail, and were released separately, resulting in the separation of FAM from BHQ and the recovery of FAM fluorescence. The released pA tail could bind with other pT_{PNK} strands, performing a binding-cleavage-release cycle, resulting in the amplification of fluorescence signal with an efficiency of nX (X is the total number of pT_{PNK} strands hybridized with the long pA tail at once, n is cycle index). Since the TdT-catalyzed elongation reaction would generate a long pA tail containing more than 500 nucleotides (see Fig. S1), this tail might hybridize with tens of pT_{PNK} strands at once, and thus giving a large X value. More important, the cleavage of each pT_{PNK} strand produced a fragment with an exposed 3'-OH end, which could also be extended by TdT to generate a new pA tail, thus triggering a new binding-cleavage-release cycle. As a result, the signal amplification cycles were continuously enlarged, giving an exponential signal amplification with a theoretical amplification efficiency of $X + X^2 + X^3 + \cdots + X^n$ (ΣX^n), which might be much higher than that of PCR (theoretical amplification efficiency: 2^n). By utilizing such a strategy, an ultra-sensitive detection of the PNK activity could be achieved. Notably, although explosive signal amplification reactions occurred in the sensing system, the detection operation could be finished in a simple "one-pot" mode.

With T4 PNK as a model, we used polyacrylamide gel electrophoresis (PAGE) and fluorescence spectrometry to verify the feasibility of the proposed strategy. As shown in Fig. S1, a clear DNA band could be only observed in the presence of both PNK and TdT (Fig. S1A), which is consistent with the proposed mechanism. The elongation product was more than 500 nt long. This result revealed that TdT would only recognize the 3'-OH end generated by the T4 PNK-catalyzed dephosphorylation. What's more, when Endo. IV was added into the system containing both PNK and TdT (Fig. S1A, Lane 3), a smeared band with 100-200 nt long appeared besides the band with ~500 nt long. According to the working mechanism shown in Scheme 1, the smeared band might be caused by TdT-catalyzed elongation of cleavage products of pT_{PNK} by Endo. IV, thus indicating the existence of the proposed exponential amplification process. The conclusion obtained from fluorescent spectrometry is consistent with PAGE. As shown in Fig. S1B, a significant increase of the fluorescent signal can be observed only in the presence of all components. To further demonstrate the proposed exponential signal amplification process, two sensing systems were prepared. In these two systems, T4 PNK and TdT were added to trigger TdT-catalyzed elongation reaction first. 60 min later, Endo. IV was added to trigger the subsequent cleavage reaction of pT_{PNK} strands. However, in one of the systems, an enzyme inactivation step (the reaction solution was heated at 85 °C for 20 min to inactivate the TdT) was introduced before the addition of Endo. IV. In the other system, no heating step was included. As shown in Fig. S1C, the non-heat system showed much higher fluorescence signal than the heated one, suggesting active TdT plays an important role after Endo. IV addition, which is consistent with the proposed mechanism that the conjugation of TdT and Endo. IV would significantly increase the efficiency of the PARTIP signal amplification.

After confirming the feasibility of PARTIP strategy, we investigated the optimal condition for PARTIP working, including the concentrations of BSA, pT_{PNK}, dATP, TdT, and Endo. IV. Comparing the signal-to-noise ratio under different conditions (see Fig. S2 to S6 for details), we finally obtained the optimized reaction condition is 500 nM of pT_{PNK}, 2 mM dATP, 10 U TdT, 5U Endo. IV and 200 μg mL^{-1} BSA in 1×TdT buffer (50 mM potassium acetate, 20 mM tris-acetate, 10 mM magnesium acetate, pH 7.9) supplemented with 250 μM $CoCl_2$ as a total volume of 25 μL.

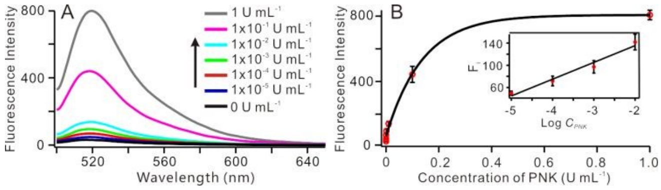

Figure 1: The PNK activity assay. (A) The fluorescent spectrum in response to different concentration of PNK. (B) Variance of the fluorescence intensity with the concentration of the PNK in a range of 1×10^{-5} to 1 U mL^{-1}. The insert shows the linear relationship between the fluorescence intensity and the logarithm of the concentration of the PNK in the range of 1×10^{-5} to 1×10^{-2} U mL^{-1}.

Under the optimized condition, we analyzed the sensitivity of PARTIP in PNK activity detection. We measured the fluorescence spectra at various concentrations of T4 PNK. The fluorescence intensity at 520 nm gradually enhanced during the increase of T4 PNK concentrations from 10^{-5} to 1 U mL^{-1} (Fig. 1A). In logarithmic scales, the fluorescence intensity exhibited a linear correlation with the concentrations of T4 PNK over a range from 10^{-5} to 10^{-2} U mL^{-1} (Fig. 2B, insert). The regression equation is F_i=195.9+30.23×logC_{PNK} with a correlation coefficient of 0.970, where F_i and C_{PNK} represent the fluorescence intensity and the T4 PNK concentration, respectively. The limit of detection (LOD) was estimated to be 3.5×10^{-6} U mL^{-1}. Notably, the LOD of this proposed sensing platform is the lowest as far as our knowledge (see Table S1). What's more, the selectivity of T4 PNK targeted PARTIP was also investigated. We employed BSA, endonuclease DpnI, methyltransferase M.SssI, and T4 ligase as the competitive proteins and enzymes. As shown in Fig. S7, the increase of the fluorescence signal was observed only in the presence of T4 PNK, revealing the excellent selectivity of the PARTIP towards the target.

Our simple one-pot signal amplification strategy makes real-time detection mode possible, in which the amplified fluorescence signal is monitored synchronously during amplification reaction. Such a real-time detection operation could be achieved conveniently using a commercial instrument (e.g. Real-Time PCR instrument). Fig. S8 showed the fluorescence intensity (F) vs reaction time (RT) curves collected at different PNK concentrations from10^{-5} to 1 U mL^{-1}. In logarithmic scale, a linear relationship was constructed between the RT_t values and the concentrations of PNK

in a wide range of 10^{-5} to 10^{-1} U mL^{-1} (See SI for more details). Such a result indicated that the PARTIP performed well in the real-time detection mode, and PNK concentration as low as 1×10^{-5} U mL^{-1} could be easily identified from those of the blank control. Compare to the end-point mode, the real-time one has simplified operation, better automation and higher throughput, thus promoting the application of the PARTIP in clinical diagnosis and prognosis.

Furthermore, the screening of PNK inhibitor by the proposed PARTIP has also been demonstrated. We used $(NH_4)_2SO_4$ and Na_2HPO_4, two of the well-known inhibitors of PNK[21, 28, 42], as the model. As shown in Fig. S9 & S10, the calculated half maximal inhibition concentrations (IC_{50}) were 13.0 mM and 11.6 mM for $(NH_4)_2SO_4$ and Na_2HPO_4, respectively. The values were consistent with those obtained by the reported methods such as the T7-exonuclease-assisted dual amplification and the magnetic-separated rolling cycle amplification[43, 44]. This result revealed that PARTIP performed well for screening PNK inhibitors and evaluating their inhibitory capacities. Because PNK has been proved to be activated in many DNA damage repair pathways[9], and recent research reported that PNK inhibitor could increase the efficiency of the existing therapy for cancers[44, 45], our sensing platform, which is available for the inhibitor screening, holds great potential in pharmacological applications.

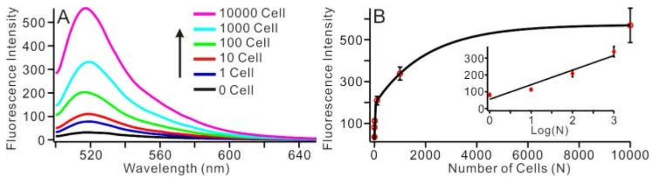

Figure 2: The PNK activity assay in HeLa cell lysate. (A) The fluorescent spectrum in response to lysates extracted from different amount of Hela cells, (B) Variance of the fluorescence intensity with the lysates extracted from different amount of Hela cells in a range of 1 to 1x104. The insert shows the linear relationship between the fluorescence intensity and the logarithm of the number of cells.

To verify the potential applications of the proposed PARTIP in naturally complex biological samples, we analyzed PNK activity in lysate of HeLa cells. As shown in Fig. S11, endogenous active PNK triggered fluorescence intensity increase was first confirmed (See SI for more details). Further, the sensitivity of PARTIP for PNK activity quantitation in HeLa cell lysate was investigated. According to the fluorescence responses to the lysate extracted from different amount of HeLa Cells (Fig. 2), a good linear relationship was constructed between the fluorescence intensity and the logarithm of the number of cells in a range of 1 to 10^3 cells, the linear regression equation was calculated as $F_i=55.2+86.7\times\log N$ (N is the number of HeLa cells), with a correlation coefficient of 0.938. This result indicated that the proposed PARTIP could sensitively detect endogenous PNK activity as low as single-cell level. According to the results in Fig. 1 and Fig. 2, we could estimate the PNK activity in HeLa cells was ~1.7×10^{-4} U per cell. This value was consistent with the result reported recently[44], demonstrating that the proposed PARTIP performed well in the application of enzyme activity assay in natural biological samples.

It is worth to note that the signal amplification process in our proposed strategy is initiated just based on target-triggered exposure of 3'-OH ends of DNA oligonucleotides. In fact, many bioprocesses may cause such an exposing of 3'-OH, thus the PARTIP can be easily extended to the detection of different biomolecules after simple modification. For instance, DNAzyme catalyzed DNA truncation, uracil specified UDG or sequence targeted methyltransferase assisted DNA cleavage[46, 47]. As an example, we designed another PARTIP for Dam Methyltransferase (Dam MTase) activity analysis, MTase may selectively catalyze the methylation of DNA with special sequence, and the aberrant MTase activities is reported to be relate with variety types of cancers including breast, prostate, lung, liver and colon cancers[48-50]. The working mechanism is shown in Fig. S12. With simple modification of the pT_{PNK}, new substrate pT_{Dam} has been constructed for the Dam MTase reorganization. The methylation of the pT_{Dam} will lead a specific enzyme cleavage thus exposing the 3'-OH end of the oligo. Then the TdT/Endo. IV assisted signal amplification would proceed similarly as the PNK assay (See SI for more details).

The feasibility of the proposed Dam MTase sensing strategy was verified through PAGE and fluorescent assay (Fig. S13). The result revealed that the signal amplification processes could be initiated only in the presence of Dam MTase (See SI for more details). We then investigated the sensitivity of the new PARTIP for the detection of Dam MTase activity. As shown in Fig. 3, the fluorescence intensity gradually enhanced during the increase of Dam MTase concentration from 4×10^{-4} to 40 U mL^{-1}. Similar to the PNK assay, the fluorescence intensity exhibited a linear correlation with the concentrations of Dam MTase over a range from 4×10^{-4} to 4 U mL^{-1} in logarithmic scales (Fig. 3B, insert). The regression equation is $F_i=389.5+91.81\times\log C_{Dam}$ with a correlation coefficient of 0.988. The LOD was estimated to be 1.1×10^{-4} U mL^{-1}.

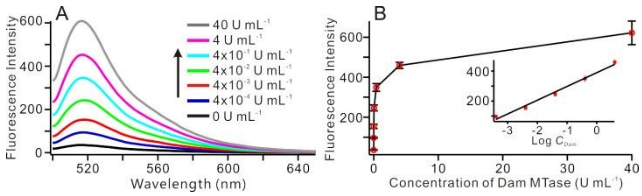

Figure 3: The Dam MTase activity assay. (A) The fluorescence spectra of the sensing system containing different concentrations of Dam MTase. (B) Variance of the fluorescence intensity at 520 nm with the concentration of the Dam MTase in a range of 4×10^{-4} to 40 U mL^{-1}. The insert shows the linear relationship between the fluorescence intensity and the logarithm of Dam MTase concentration in the range of 4×10^{-4} to 4 U mL^{-1}.

Using another methyltransferase M.SssI, which may catalyze the methylation of cytosine in CpG region and endonuclease EcoRI as the competitive enzymes, the Dam MTase targeted PARTIP was demonstrated with good selectivity for the Dam MTase detection (see Fig. S14A & B for the detailed results). In addition, we measured the fluorescent intensity in the presence of 5-fluorouracil or gentamycin, two commonly used Dam MTase inhibitors. When 1 μM 5-Fluorouracil or 10 μM gentamycin (the concentrations were close to their IC_{50} values reported in previous research[26, 44]) were added in, the calculated relative activities of Dam MTase were reduced to 41.0% and 48.9%. (see Fig. S14C & D for detailed results). This result indicated that the new PARTIP is capable for the Dam MTase inhibitor screening assay.

Finally, we demonstrated that the detection of Dam MTase activity can be achieved through the real-time detection mode. As shown in Fig. S15, a concentration of Dam MTase as low as 4×10^{-4} U mL^{-1} can be easily identified from the blank control, and a linear relationship was obtained on the logarithmic scale in a range of 4×10^{-4} to 4 U mL^{-1}. The linear regression equation was calculated as $RT_t=40.0-18.0\times\log C_{Dam}$, with a correlation coefficient of 0.999. All above results indicated this PARTIP performed well for one-pot detection of Dam MTase.

In summary, we proposed a new strategy to construct sensing platform named as PARTIP for highly sensitive quantitation of

diverse biologically important molecules. In this strategy, only one substrate, which plays three roles of probe, signal amplifier and signal output, was used. Due to the alternant initiation of TdT-catalyzed substrate extension and Endo. IV-catalyzed substrate cleavage, the signal output of the sensing platforms can be amplified in an exponential mode with a theoretical amplification efficiency of ΣX^n. As a result, PARTIP showed great sensitivity for the specific targets. The PNK activity detection in the lysate from individual HeLa cell can be precisely achieved. The ultra-simple "one-pot" detection mode guaranteed the potential of PARTIP in general application. Overall, our proposed strategy provides a universal tool for clinical diagnosis, pharmacological analysis and disease therapic assay.

Conflicts of interest

There are no conflicts to declare.

Notes and references

1. C. Sutherland, Y. X. Cui, H. B. Mao and L. H. Hurley, J. Am. Chem. Soc., 2016, 138, 14138-14151.
2. M. Zeraati, D. B. Langley, P. Schofield, A. L. Moye, R. Rouet, W. E. Hughes, T. M. Bryan, M. E. Dinger and D. Christ, Nat. Chem., 2018, 10, 631-637.
3. A. B. Foraker, C. M. Khantwal and P. W. Swaan, Adv. Drug Deliv. Rev., 2003, 55, 1467-1483.
4. A. Renzoni, F. Zino and E. Franchi, Environ. Res., 1998, 77, 68-72.
5. V. Ambros, Nature, 2004, 431, 350-355.
6. K. D. Robertson, Oncogene, 2001, 20, 3139-3155.
7. C. B. Ma and E. S. Yeung, Anal. Bioanal. Chem., 2010, 397, 2279-2284.
8. Z. W. Tang, K. M. Wang, W. H. Tan, C. B. Ma, J. Li, L. F. Liu, Q. P. Guo and X. X. Meng, Nucleic Acids Res., 2005, 33.
9. C. J. Whitehouse, R. M. Taylor, A. Thistlethwaite, H. Zhang, F. Karimi-Busheri, D. D. Lasko, M. Weinfeld and K. W. Caldecott, Cell, 2001, 104, 107-117.
10. D. P. Bartel, Cell, 2009, 136, 215-233.
11. S. Ikeda, S. W. Kong, J. Lu, E. Bisping, H. Zhang, P. D. Allen, T. R. Golub, B. Pieske and W. T. Pu, Physiol. Genomics, 2007, 31, 367-373.
12. Y. Yamamoto, N. Kosaka, M. Tanaka, F. Koizumi, Y. Kanai, T. Mizutani, Y. Murakami, M. Kuroda, A. Miyajima, T. Kato and T. Ochiya, Biomarkers, 2009, 14, 529-538.
13. M. V. Iorio, M. Ferracin, C. G. Liu, A. Veronese, R. Spizzo, S. Sabbioni, E. Magri, M. Pedriali, M. Fabbri, M. Campiglio, S. Menard, J. P. Palazzo, A. Rosenberg, P. Musiani, S. Volinia, I. Nenci, G. A. Calin, P. Querzoli, M. Negrini and C. M. Croce, Cancer Res., 2005, 65, 7065-7070.
14. L.-M. Zhang, Y.-X. Cui, L.-N. Zhu, J.-Q. Chu and D.-M. Kong, Nucleic Acids Res., 2019.
15. S. Tombelli, M. Minunni and A. Mascini, Biosens. Bioelectron., 2005, 20, 2424-2434.
16. Y. Tang, B. Lu, Z. Zhu and B. Li, Chem. Sci., 2018, 9, 760-769.
17. M. S. Reid, X. C. Le and H. Q. Zhang, Angewandte Chemie-International Edition, 2018, 57, 11856-11866.
18. G. Z. Zhu, R. Hu, Z. L. Zhao, Z. Chen, X. B. Zhang and W. H. Tan, J. Am. Chem. Soc., 2013, 135, 16438-16445.
19. W. Li, Z. L. Liu, H. Lin, Z. Nie and J. H. Chen, Anal. Chem., 2010, 82, 1935-1941.
20. M. Thomas and R. W. Davis, Journal of molecular biology, 1975, 91, 315-328.
21. L.-j. Wang, Q. Zhang, B. Tang and C.-y. Zhang, Anal. Chem., 2017, 89, 7255-7261.
22. W. Zhu, Z. Zhao, Z. Li, J. Jiang, G. Shen and R. Yu, J. Mat. Chem. B, 2013, 1, 361-367.
23. R. J. Wood, J. C. McKelvie, M. D. Maynard-Smith and P. L. Roach, Nucleic Acids Res., 2010, 38, e107.
24. H. Zhou, J. Liu, J.-J. Xu, S.-S. Zhang and H.-Y. Chen, Chem. Soc. Rev., 2018, 47, 1996-2019.
25. Q. Wei, J. Huang, J. Li, J. Wang, X. Yang, J. Liu and K. Wang, Chem. Sci., 2018, 9, 7802-7808.
26. Y. X. Cui, X. N. Feng, Y. X. Wang, H. Y. Pan, H. Pan and D. M. Kong, Chem. Sci., 2019, 10, 2290-2297.
27. Y. C. Du, Y. X. Cui, X. Y. Li, G. Y. Sun, Y. P. Zhang, A. N. Tang, K. Kim and D. M. Kong, Anal. Chem., 2018, 90, 8629-8634.
28. N.-N. Sun, R.-M. Kong, F. Qu, X. Zhang, S. Zhang and J. You, Analyst, 2015, 140, 1827-1831.
29. W. L. Cui, L. Wang, X. W. Xu, Y. Wang and W. Jiang, Sens. Actuator B-Chem., 2017, 244, 599-605.
30. W. H. Wu, T. Zhang, D. Han, H. L. Fan, G. Z. Zhu, X. Ding, C. C. Wu, M. X. You, L. P. Qiu, J. Li, L. Q. Zhang, X. Lian, R. Hu, Y. Mu, J. G. Zhou and W. H. Tan, Chem. Sci., 2018, 9, 3050-3055.
31. Y. X. Chu, A. P. Deng, W. J. Wang and J. J. Zhu, Anal. Chem., 2019, 91, 3619-3627.
32. H. D. Van Guilder, K. E. Vrana and W. M. Freeman, Biotechniques, 2008, 44, 619-626.
33. C. S. Zhang, J. L. Xu, W. L. Ma and W. L. Zheng, Biotechnol. Adv., 2006, 24, 243-284.
34. L. J. Wang, X. Han, C. C. Li and C. Y. Zhang, Chem. Sci., 2018, 9, 6053-6061.
35. S. Rauf, J. J. Gooding, K. Akhtar, M. A. Ghauri, M. Rahman, M. A. Anwar and A. M. Khalid, J. Pharm. Biomed. Anal., 2005, 37, 205-217.
36. C. Frauendorf, F. Hausch, I. Rohl, A. Lichte, S. Vonhoff and S. Klussmann, Nucleic Acids Research, 2003, 31.
37. F. Karimi-Busheri, A. Rasouli-Nia, J. Allalunis-Turner and M. Weinfeld, Cancer research, 2007, 67, 6619-6625.
38. S. Liu, T. Liu and L. Wang, Chemical Communications, 2015, 51, 176-179.
39. W. Reik, W. Dean and J. Walter, Science, 2001, 293, 1089-1093.
40. S. Palluk, D. H. Arlow, T. de Rond, S. Barthel, J. S. Kang, R. Bector, H. M. Baghdassarian, A. N. Truong, P. W. Kim, A. K. Singh, N. J. Hillson and J. D. Keasling, Nature Biotechnology, 2018, 36, 645-650.
41. M. Zuker, Nucleic Acids Res., 2003, 31, 3406-3415.
42. V. Cameron and O. C. Uhlenbeck, Biochemistry, 1977, 16, 5120-5126.
43. X. Li, X. W. Xu, J. Song, Q. W. Xue, C. Z. Li and W. Jiang, Biosens. Bioelectron., 2017, 91, 631-636.
44. X.-Y. Li, Y.-C. Du, Y.-N. Pan, L.-L. Su, S. Shi, S.-Y. Wang, A.-N. Tang, K. Kim and D.-M. Kong, Chem. Commun., 2018, 54, 13841-13844.
45. S. L. Allinson, Future Oncol., 2010, 6, 1031-1042.
46. L. Zou, Q. Wu, Y. Zhou, X. Gong, X. Liu and F. Wang, Chemical communications (Cambridge, England), 2019.
47. C. X. Li, H. M. Wang, J. H. Shang, X. Q. Liu, B. F. Yuan and F. Wang, ACS Sens., 2018, 3, 2359-2366.
48. P. W. Laird, Nature Reviews Cancer, 2003, 3, 253-266.
49. D. K. Vanaja, M. Ehrich, D. Van den Boom, J. C. Cheville, R. J. Karnes, D. J. Tindall, C. R. Cantor and C. Y. F. Young, Cancer Invest., 2009, 27, 549-560.
50. K. Miyamoto, T. Fukutomi, S. Akashi-Tanaka, T. Hasegawa, T. Asahara, T. Sugimura and T. Ushijima, Int. J. Cancer, 2005, 116, 407-414.

View Article Online DOI: 10.1039/C9CC03758F